

WL-TR-96-1112

# OPTICAL SURFACE ANALYSIS



**Jeff L. Brown**

**August 1996  
Final Report for Period Oct 1982 through Sep 1992**

Approved for public release; distribution is unlimited.

**Avionics Directorate  
Wright Laboratory  
Air Force Materiel Command  
Wright-Patterson Air Force Base, OH 45433-7322**

**20000406 094**

*DTIC QUALITY INSPECTED 1*

## NOTICE

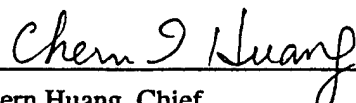
WHEN GOVERNMENT DRAWINGS, SPECIFICATIONS, OR OTHER DATA ARE USED FOR ANY PURPOSE OTHER THAN IN CONNECTION WITH A DEFINITELY GOVERNMENT-RELATED PROCUREMENT, THE UNITED STATES GOVERNMENT INCURS NO RESPONSIBILITY OR ANY OBLIGATION WHATSOEVER. THE FACT THAT THE GOVERNMENT MAY HAVE FORMULATED OR IN ANYWAY SUPPLIED THE SAID DRAWINGS, SPECIFICATIONS, OR OTHER DATA, IS NOT TO BE REGARDED BY IMPLICATION, OR OTHERWISE IN ANY MANNER CONSTRUED, AS LICENSING THE HOLDER, OR ANY OTHER PERSON OR CORPORATION; OR AS CONVEYING ANY RIGHTS OR PERMISSION TO MANUFACTURE, USE, OR SELL ANY PATENTED INVENTION THAT MAY IN ANY WAY BE RELATED THERETO.

This report is releasable to the National Technical Information Service (NTIS). At NTIS, it will be available to the general public, including foreign nations.

This technical report has been reviewed and is approved for publication.



Jeff L. Brown  
Principal Investigator  
Heterojunction Physics Branch



Chern Huang, Chief  
Heterojunction Physics Branch  
Electron Devices Division



Tim Kemerley, Chief  
Electron Devices Division  
Avionics Directorate

If your address has changed, if you wish to be removed from our mailing list, or if the addressee is no longer employed by your organization, please notify, WL/AADP BLDG 620, 2241 Avionics Circle RM C2G69, Wright-Patterson AFB OH 45433-7322 to help us maintain a current mailing list.

Copies of this report should not be returned unless return is required by security considerations, contractual obligations, or notice on a specific document.

## REPORT DOCUMENTATION PAGE

Form Approved  
OMB No. 0704-0188

Public reporting burden for this collection of information is estimated to average 1 hour per response, including the time for reviewing instructions, searching existing data sources, gathering and maintaining the data needed, and completing and reviewing the collection of information. Send comments regarding this burden estimate or any other aspect of this collection of information, including suggestions for reducing this burden, to Washington Headquarters Services, Directorate for Information Operations and Reports, 1215 Jefferson Davis Highway, Suite 1204, Arlington, VA 22202-4302, and to the Office of Management and Budget, Paperwork Reduction Project (0704-0188), Washington, DC 20503.

1. AGENCY USE ONLY (Leave blank)	2. REPORT DATE	3. REPORT TYPE AND DATES COVERED	
	Aug 1996	Final 10/01/82--09/30/92	
4. TITLE AND SUBTITLE		5. FUNDING NUMBERS	
OPTICAL SURFACE ANALYSIS		PE: 62204F PR: 2001 TA: 05 WU: 07	
6. AUTHOR(S)			
Jeff L. Brown			
7. PERFORMING ORGANIZATION NAME(S) AND ADDRESS(ES)		8. PERFORMING ORGANIZATION REPORT NUMBER	
Avionics Directorate Wright Laboratory (ASC) Air Force Materiel Command Wright-Patterson AFB OH 45433-7320			
9. SPONSORING/MONITORING AGENCY NAME(S) AND ADDRESS(ES)		10. SPONSORING/MONITORING AGENCY REPORT NUMBER	
Avionics Directorate Wright Laboratory (ASC) Air Force Materiel Command Wright-Patterson AFB OH 45433-7320 POC: Jeff Brown, WL/AADP, WPAFB OH; 937-255-4736		WL-TR-96-1112	
11. SUPPLEMENTARY NOTES			
This is an in-house research report			
12a. DISTRIBUTION AVAILABILITY STATEMENT		12b. DISTRIBUTION CODE	
Approved for public release; distribution is unlimited			
13. ABSTRACT (Maximum 200 words)			
This report documents work that has centered around the continued development of a unique scatterometer and its transition to semiconductor materials characterization. A brief history of this lengthy project is contained in the Preface. Following an introduction in Section 1, Section 2 explains some background to this work and some of the motivations for pursuing it. Section 3 presents the work done to modernize and otherwise improve the scatterometer as it existed at the beginning of this work unit. Section 4 presents the work done to increase the capabilities of the scatterometer to include such things as multiple wavelength scattering, polarization control, 4" diameter sample capability, and improved alignment and automation features. Section 5 presents the design and initial testing of a scatterometer that has some distinct advantages over the current system. Section 6 presents initial work in approaching the problem of quantifying subsurface scatter. The remaining sections describe various important sub-tasks and miscellaneous items, concluding with a section on the direction in which future work will likely go as similar work continues under other work units.			
14. SUBJECT TERMS		15. NUMBER OF PAGES	
Scatterometry, scatterometer, light scattering, optical surface characterization, polishing, semiconductor substrates, gallium arsenide		68	
16. PRICE CODE			
17. SECURITY CLASSIFICATION OF REPORT	18. SECURITY CLASSIFICATION OF THIS PAGE	19. SECURITY CLASSIFICATION OF ABSTRACT	20. LIMITATION OF ABSTRACT
UNCLASSIFIED	UNCLASSIFIED	UNCLASSIFIED	UL

## TABLE OF CONTENTS

LIST OF ILLUSTRATIONS.....	v
PREFACE.....	vi
1. INTRODUCTION .....	1
2. BACKGROUND .....	3
3. SCATTEROMETER MODERNIZATION AND OTHER IMPROVEMENTS .....	8
3.1 Improvement of the laser beam positioning and conditioning subsystem.....	8
3.2 New computer control subsystem.....	13
3.3 New devices and interfaces .....	16
3.3.1 Motor controller .....	16
3.3.2 Power monitor.....	17
3.3.3 Photometer.....	17
3.3.4 Other .....	22
4. NEW SCATTEROMETER CAPABILITIES .....	23
4.1 Polarization control.....	23
4.2 Four-inch sample translation.....	25
4.3 New photometer .....	26
4.4 New laser sources .....	27
4.5 Additional motor-driven translations .....	28
5. NEW SCATTEROMETER DESIGN.....	30
6. SUBSURFACE SCATTER STUDIES.....	38
7. BRDF ROUND ROBIN .....	40
8. GALLIUM ARSENIDE MATERIAL MEASUREMENTS .....	46
9. SURFACE PREPARATION STUDIES .....	50
10. OTHER INSTRUMENTATION .....	52
10.1 DIC Microscope .....	52
10.2 Interferometric microscope .....	53

10.3 Scanning Probe Microscope .....	53
11. MISCELLANY .....	55
11.1 Reference materials .....	55
11.2 Alignment .....	57
11.3 Standard operating procedures .....	57
11.4 Support for various extramural projects .....	57
12. FUTURE DIRECTIONS .....	59
13. REFERENCES .....	60

## LIST OF ILLUSTRATIONS

<u>FIGURE</u>	<u>PAGE</u>
<b>Fig. 1.</b> Front view of the sample manipulator.....	34
<b>Fig. 2.</b> Side view of the fiber manipulator.....	35
<b>Fig. 3.</b> Front view of the fiber manipulator.....	36
<b>Fig. 4.</b> Side view of the sample manipulator and fiber manipulator.....	37

## PREFACE

This report summarizes the work performed under the Solid State Electronics Directorate, Wright Laboratory, in-house work unit 20010507, Optical Surface Analysis, covering the period 1 Oct 82 through 30 Sep 92.

The author of this report became involved with this work unit in Jan 1986 and became the work unit monitor and principal investigator in Aug 1987. Any official records of this work unit covering the period 1 Oct 82 through 1 Aug 87, if any ever existed, could not be located. The author is therefore relying on the recollections of Mr James Grote to fill in the time prior to 1986.

This work unit was initiated when the Ring Laser Gyro Laboratory was moved from AFWAL/AAAN-2 and became part of AFWAL/AADO-2 (Avionics Laboratory, Air Force Wright Aeronautical Laboratory) some time in 1982. At that time, the Ring Laser Gyro Laboratory was under the technical direction of Dr W. Kent Stowell, the principal investigator. This work unit supported a variety of work under the general title of Surface Studies, but was specifically aimed at studying surface imperfections of optical components suitable for use in ring laser gyroscopes and how those imperfections affected the performance of ring laser gyroscopes. This research was centered around the development and use of an instrument called a variable angle scatterometer, one of the early such instruments, and this report is concerned mainly with this topic.

At the conclusion of this work unit, the optical surface analysis work continued under work unit 20010512 in WL/ELOT. In Jan 1995, the author and the optical surface analysis laboratory were transferred to WL/AADP where they reside at the time of this writing. The current capabilities of the optical surface analysis lab are fundamentally the same as those described in this report and these capabilities support current characterization requirements of WL/AADP.

Many individuals have contributed to the work described herein. Dr W. Kent Stowell, the contractors of VTI, Inc., Jim Grote, Sam Adams, and others conceived of and/or built the original variable angle scatterometer. Judy Theodosakis, the author's immediate predecessor, operated the scatterometer and performed many experimental measurements on optical components. Virginia McMillan also operated the scatterometer and performed data analysis. During the author's tenure as principal investigator, John Hoeft wrote a completely new software control program and designed most of the modernized, computer-controlled instrument interface; Sam Adams and Sam LaForge designed and machined many of the parts for the upgraded scatterometer; Jim Grote assisted in many ways, too numerous to list here. The author wishes to thank Virginia McMillan for introducing him to the operation of the original scatterometer; Jim Grote (who knew the most about the technical details of the original scatterometer's hardware and software, especially the PDP-11 computer) for his assistance and corporate memory; John Hoeft, who became a good friend and office mate as we worked together on the scatterometer modifications; and a special thanks to Joe Brandelik for copious personal and technical advice.

This report is written with the assumption that the reader has a basic understanding of optical physics. Since this report is largely concerned with instrumentation and the results of measurements, underlying theory and detailed background is left to the references. Any introductory physics text or optics text should suffice for general background and more specialized detail is referenced in the body of this report.

## 1. INTRODUCTION

The original objective of this work unit was to establish and maintain a measurement facility capable of investigating the visible wavelength light scattering properties of ring laser gyroscope mirrors and the substrates from which these mirrors were made. One ultimate objective, which was never realized at Wright Laboratory, was to make scattering measurements *in situ* on one of the mirrors of an operating ring laser gyro, thus relating an independent physical measurement of the mirror surface with a measurement of how the mirror performed as a working optical component. The realized scatterometer instrument served as one major step toward the larger goal and in the process became a characterization instrument which proved to be of great benefit as described throughout this report. Eventually, when the ring laser gyro test bed was moved to Phillips Laboratory, the objective became one of continued development of a measurement facility for the purpose of providing non-destructive testing of surfaces in general, be they dielectric, metal, or semiconductor surfaces. The high sensitivity and spatial mapping capability of the scatterometer made it especially useful for investigating surface and near subsurface imperfections in polished semiconductor materials. A more general objective which evolved was to use the established measurement techniques and hardware to investigate basic questions related to the science of roughness and scattering measurements.

To this end, several tasks were undertaken to modernize existing equipment, increase the capabilities of the equipment, develop new scatterometer designs, and work on some of the unresolved issues in light scattering metrology, especially the quantification of subsurface scatter. Along the way, many opportunities to measure a variety of materials, to participate in collaborations with in-house and other investigators, and to support in-house research were taken advantage of.

Section 2 explains some background to this work and some of the motivations for

pursuing it. Section 3 presents the work done to modernize and otherwise improve the scatterometer as it existed at the beginning of this work unit. Section 4 presents the work done to increase the capabilities of the scatterometer to include such things as multiple wavelength scattering, polarization control, 4" diameter sample capability, and improved alignment and automation features. Section 5 presents the design and initial testing of a scatterometer that has some distinct advantages over the current system. Section 6 presents initial work in approaching the problem of quantifying subsurface scatter. The remaining sections describe various important sub-tasks and miscellaneous items, concluding with a section on the direction in which future work will likely go as similar work continues under other work units.

## 2. BACKGROUND

In the context of this report, optical surface analysis refers to optical nondestructive methods for evaluating physical surface imperfections. These imperfections include surface roughness, contamination, material nonuniformities, etc., all of which can scatter light that would otherwise obey the basic laws of optics describing reflection and refraction at an interface. Light scattered from the surface of an optical component does not directly characterize the imperfections of the surface, but the magnitude and directional distribution of the scattered light can be related to surface imperfections, such as surface roughness.

The primary tool for measuring scattered light is the scatterometer. Other optical tools for measuring surface imperfections include various types of light microscopes, optical interferometric microscopes, and optical profilometers, but the scatterometer has several advantages over these other tools. In most cases, the performance of an optical element is limited by the amount of light it scatters and the tolerable amount of scattering can become part of an optical specification regardless of what the source or sources of the scattering might be. Other tools are then useful for determining the root cause of the scattering. A second advantage of a scatterometer is that it is usually easier to automate so that a sample can be more fully characterized, both in terms of the spatial distribution of the scattered light from a given area of the surface and how the distribution varies with location on the surface. The other tools are normally used to study small areas of a surface in great detail, something that is not always relevant to how the entire optical surface will perform in practice. In addition, a scatterometer measures the average effect of the imperfections within each measurement area whose size is usually large with respect to the size of the individual imperfections. This can greatly speed up the process of characterizing a sample surface.

Thus, the scatterometer has become an important tool for characterizing optical

components. While the bulk properties of an optical component are important, the surfaces of these components usually pose the greatest challenge for controlling the amount of light the component will scatter. The surfaces are usually ground and polished after being cut from larger pieces of bulk material. The grinding and polishing is not perfect and leaves a surface that is never perfectly smooth and homogeneous. As a result, a portion of any light impinging on these surfaces can be scattered in directions other than those predicted by the Law of Reflection and Snell's Law. In general, a small amount of light will be scattered in any given direction on both sides of the surface interface.

In order to characterize a surface's light scattering nature, it is necessary to define a quantity that describes the magnitude and direction in which light will be scattered from a surface as a function of incident magnitude, direction, and wavelength of any light impinging on the surface interface. F. E. Nicodemus<sup>1</sup> introduced the concept of directional reflectance in terms of radiometric quantities and later Nicodemus, et al.,<sup>2</sup> defined the bidirectional spectral-reflectance distribution function. The latter quantity is a property of the surface in question and is the directional reflectance per unit solid angle of collected scattered light. When dealing with monochromatic light sources, which is usually the case, the bidirectional reflectance distribution function (BRDF) becomes the quantity of interest. The precise nomenclature and geometry of what is essentially a radiometric description of reflection, generalized to describe both diffuse and specular reflection, is cumbersome to use in experimentation. Assumptions made in the derivation of BRDF are rarely valid for the measurement of real surfaces, so it has become convenient to define the bidirectional scatter distribution function (BSDF)<sup>3</sup> which embodies the geometry and nomenclature of the formal BRDF, but recognizes the fact that real measurements of differential quantities are only approximations.

The BSDF is defined as

$$BSDF(\theta_i, \phi_i; \theta_s, \phi_s) \equiv \frac{P_s / \Omega_s}{P_i \cos \theta_s} \quad (1)$$

where  $P_s$  is the power collected by an aperture subtending a solid angle  $\Omega_s$  in the direction given by  $(\theta_s, \phi_s)$  and  $P_i$  is the power of a well collimated beam of light incident from the direction  $(\theta_i, \phi_i)$ . The  $\cos\theta_s$  term is sometimes dropped, but the definition above is used throughout this work. BSDF is a generic term encompassing reflective, transmissive, and volume scattering. It is common to refer to BRDF as a subset of BSDF and to use the form of Eq. (1) instead of the more formal differential form given by Nicodemus. This usage is used throughout this report. For a detailed discussion of the preceding issues, and optical scattering in general, see the text by Stover.<sup>3</sup>

The earliest form of scatterometer measured total integrated scatter (TIS) which, as the name implies, integrates the majority of light scattered from a spot illuminated by a laser beam or other collimated light source.<sup>4</sup> Any specularly reflected light is not included in the integration. This type of characterization is the most basic type of scattering measurement, but it cannot discern the directional scattering nature of many types of imperfections which can give the scattering distribution a nonsymmetrical shape.

Subsequently, instruments were designed which could measure BRDF. Since BRDF is a function of the direction of incident and scattered light, various scatterometers were capable of varying at least one of these directions. A common solution was an in-plane scatterometer which could scan a detector in the plane of incidence of an incident laser beam. Often the incident beam direction could be varied as well. One of these early scatterometers was built for the purpose of evaluating ring laser gyroscope mirrors in the Ring Laser Gyro Laboratory at Wright-Patterson AFB. This scatterometer was called a variable angle scatterometer (VAS) and is described in some detail in a paper by Orazio, Stowell, and Silva.<sup>5</sup> A more detailed description of the VAS is contained in an unpublished report by Orazio, Sledge, and Silva. Several papers also reported on the results of measurements obtained from the VAS.<sup>6,7,8</sup>

The VAS, as designed, was an in-plane, single wavelength scatterometer with several

unique features which distinguished it from other contemporary scatterometers, and to this day most of these features remain unique. The VAS had a fixed detector and the scatter angle was varied by rotating a large table which contained the sample mount and translation system, and the laser and its beam directing optics. The sample and laser rotated as a unit via a stepping motor to keep the incident angle constant. The laser beam incident angle was varied by rotation of the sample mount with respect to the laser and independent of the large rotation table. A second unique feature was a rotation stage mounted behind two orthogonal linear translation stages which comprised the sample manipulation capability. All of these stages were driven by stepping motors. With the rotary stage behind the translation stages, a rotary scan could be taken for any point on a sample surface by measuring scatter as a function of sample rotation. A third unique feature was the use of a Pritchard photometer which allowed for unambiguous alignment of the detector field stop on the sample, and, to a certain extent, gave the VAS its extreme sensitivity.

The literature referenced in the previous paragraphs describes the state of the VAS and the work being done in surface analysis at the time this work unit was initiated. Similar work continued and steadily progressed toward characterization of semiconductor substrates and epitaxial material grown on semiconductor substrates by various methods. The remainder of this section discusses the motivation behind pursuing this work.

Previous investigations have shown the usefulness of light scatter measurements for characterizing surfaces. Quantitative and qualitative information about the surface interface as well as the region just below the interface (subsurface) can be obtained. In the case of transparent substances, even bulk scattering properties can be measured. Measurements performed by light scattering techniques are non-destructive.

Several issues in the area of light scattering have been of interest for many years. These include the importance of wavelength scaling and polarization dependence in scatter measurements, subsurface defect detection, and even standardization of measurement quantities

and methods. These issues, and the applicability of light scatter measurements to GaAs research, motivated this work.

Early work in light scattering metrology involved its use as a quantitative measure of surface finish on polished glass. This information proved useful as feedback for polishers, especially those producing the highly polished surfaces necessary for advanced applications, e.g. mirrors for ring laser gyroscopes. As the study of imperfections in semiconductor materials began to take on increased importance, light scattering was seen as a potentially useful tool for this material study. Its non-destructive nature and extreme sensitivity to small changes in a material, coupled with its ability to cover large surface areas with more resolution than was typical for most surface characterization methods, made it a good compliment to other semiconductor characterization techniques already in use in semiconductor research and development.

### 3. SCATTEROMETER MODERNIZATION AND OTHER IMPROVEMENTS

At the time the VAS was constructed, it was generally necessary to build many components of a complex scientific instrument from scratch in the laboratory or to have the components built to in-house designs and specifications. Aside from the PDP-11 mini-computer, most of the electronic components for computer control of the VAS fell into this category. In addition, major parts of the laser beam positioning and conditioning subsystem were manufactured in-house with rudimentary alignment features. One of the major goals of this work unit was to improve and modernize the VAS to take advantage of new products on the market and especially to take advantage of emerging personal computer products and electronic interfacing and software designed for personal computers.

#### 3.1 Improvement of the laser beam positioning and conditioning subsystem

The laser beam positioning and conditioning subsystem consisted of a laser, beam steering optics, a spatial filter and collimator, a beamsplitter, and a beam absorber. The performance of this subsystem was adequate but difficult to align. The alignment procedures are intricate and will not be described here, but the difficulty in alignment stemmed from inadequate translation and tilt control of the optical elements in the subsystem. Four modifications were made to this subsystem which made alignment more precise and predictable. These modifications involved adding a translation stage for the beam elevation adjustment, repositioning the beamsplitter and power monitor, adding tilt and translation stages to the spatial filter and collimator assembly, and redesigning the spatial filter and collimator assembly itself.

The first modification was the addition of a vertical translation stage with a fine pitch adjustment screw to the upper mirror of the Newport Model 675 beam steering instrument. This added finer positioning control to the rack and pinion adjustment of the height of the upper

mirror, thus allowing finer control of the elevation of the beam incident on the sample. It also provided more stable elevation adjustments since adjustment of the rack and pinion can also cause small tilt and pointing changes at the same time. The addition of the translation stage required that a spacer be added to the lower mirror and that the position of the spatial filter and collimator assembly be moved somewhat to accommodate the change in mounting position of the upper mirror.

The second modification involved repositioning of the beamsplitter and power monitor. The original position of these components was just after the spatial filter and collimator and they were housed as a unit with the spatial filter and collimator for the purpose of splitting off part of the beam for beam power monitoring. This positioned the beamsplitter as the final optical element in the beam path just prior to the sample surface. A drawback of this arrangement is that the beamsplitter, consisting of a thin plate of glass, deviates the beam slightly. This in turn causes some difficulties during certain stages of the alignment process. The reason for placement of the beamsplitter after the beam conditioning optics is that the optical attenuation of all the elements preceding the beamsplitter can be ignored and, if the reflectivity of the beamsplitter is known and the beam power monitor is calibrated, the actual power on the sample can be easily determined. However, since the incident power is incorporated into the scale factor for converting measurements to units of BRDF, and since the scale factor is determined by measurement of a known scatterer, knowledge of the actual incident power is not necessary. The power monitor then serves only to account for small fluctuations in laser power. Therefore, the beamsplitter and power monitor could be repositioned near the output of the laser itself.

This solution was accomplished by placing the beamsplitter plate into the beam path near the laser output and directing the beam onto the power monitor detector. The beamsplitter and power monitor were no longer housed in a single unit, but instead were held by separate post mounting platforms. This arrangement is not optimum and ideally the beamsplitter and power

monitor detector should be housed in a single unit for stability and protection of the optical elements. While solving the alignment difficulties, the current post mounting arrangement has the drawback of being prone to misalignment by bumping during normal operation. In practice, however, this hasn't been a serious problem.

The third modification to the laser beam positioning and conditioning subsystem was the addition of tilt and translation stages to the spatial filter and collimator assembly. During alignment, the raw beam is first positioned and pointed in the proper direction. One of the last steps is to place the spatial filter and collimator assembly into the beam and align the assembly such that the beam is positioned and pointed identically to the raw beam. In order to do this, the entire assembly needs to have four degrees of freedom - horizontal and vertical translations, and yaw and pitch tilts. The drawback to the previous method was that the translations and tilts were accomplished using set screws.

The solution to this drawback was to replace the stand upon which the spatial filter and collimator were mounted with, from the bottom up, a short spacer and mounting block, followed by a horizontal translation stage, in turn followed by a vertical translation stage, in turn followed by a tilt table designed to provide rotation about the three coordinate axes. This type of tilt table is sometimes referred to as a prism table. A small optical bench containing the redesigned spatial filter and collimator was then mounted on the tilt table. The tilt table provided the yaw and pitch tilts necessary for alignment of the spatial filter and collimator in the beam. The roll tilt provided by the tilt table was locked and not used.

This solution was much easier to use during alignments because each adjustment knob controlled a single degree of freedom whereas, in the previous arrangement, a combination of set screw adjustments was required for a single translation or tilt. This solution had some drawbacks, however. The locking nuts on the tilt adjustment knobs are difficult to tighten without causing additional tilt. During alignment, a trial and error approach is used in which a combination of an

adjustment and a locking action are performed until the locked position produces the desired tilt adjustment. A tilt table with a better locking mechanism would solve this problem.

The fourth modification involved redesigning the spatial filter and collimator assembly itself. A spatial filter is used to remove high spatial frequency noise from a laser beam. This involves focusing the beam to a small spot and passing the beam through a pinhole which blocks the high frequency spatial noise and cleans up the beam profile. Generally, the beam is then collimated again with an appropriate lens or lens system. Adequate beam conditioning was obtained in this way on the VAS using a 1.5x beam expander followed by a 10x microscope objective, a magnetically mounted pinhole with translators, and a second 10x microscope objective. Both microscope objectives could be adjusted in an axial direction for focusing. The first objective requires adjustment in order to place the focused beam waist in the plane of the pinhole. The second objective requires adjustment in order to place the collimated beam waist in the sample plane.

The major drawback in this assembly was that there were no lateral or tilt adjustments for the optical elements of the spatial filter and collimator except for positioning of the pinhole. Microscope objectives and mounting threads usually are not critically aligned for laser beam use and in this case the objectives contained two lens. Tilt misalignments of these types of optical elements usually means that the laser beam will not traverse a single straight line path through the assembly. Some allowances were made in the assembly for the addition of shims to help correct this deficiency, but the shimming process was not intended for routine alignment. Rather, it was to be a rare occurrence. However, if the alignment of the optical elements was ever disturbed, an extremely tedious alignment was required.

Ideally, in order to place the spatial filter and collimator assembly into the raw aligned beam and maintain the positioning and pointing of that beam, the optical elements of the spatial filter and collimator need to be bore sighted; that is, each element must be aligned to a reference

beam. In order to accomplish this, each element must be able to be positioned relative to the other elements. Relative tilts can also be important; but in the solution discussed below, relative tilts can be ignored.

In order to obtain a spatial filter and collimator assembly that could easily be bench aligned, the previous design was thrown out and a new design devised. An experiment was conducted to find an appropriate combination of optical elements that would accomplish nearly the same function as the original, but with fewer components and with the ability to vary the spot size of the beam over a small range while always keeping the beam collimated. In addition, a solution with fewer components was sought so that a minimum number of linear translation stages would satisfy the independent translation requirements in order to conserve space. A solution was found which had the following components: 1) the beam expander and the first microscope objective were replaced with a single 10x/0.25 N.A. microscope objective mounted on a single linear translation stage for focus adjustment, 2) the existing pinhole was replaced with a  $25\text{ }\mu\text{m}$  pinhole while retaining the original magnetic pinhole mount and translators, 3) the second 10x microscope objective was replaced with a 10x microscope objective with one of the lenses removed and mounted on three orthogonal translation stages. In this way, both the pinhole and the second objective could be translated laterally relative to the first objective and the second objective could be adjusted to vary the beam spot size on the sample. This combination, while not capable of obtaining as small a spot size in the sample plane as the original design, is capable of obtaining beam spot diameters in the approximate range from 0.25-1.00 mm such that the sample plane is always within the collimated range (Rayleigh range). This design was verified by laser propagation calculations and experimental measurements using the translating wire method.

With this new design, the spatial filter and collimator assembly, mounted on top of the tilt table, could be bore sighted on an optical bench with a reference laser beam and then the entire assembly could be mounted on the scatterometer and aligned to the raw beam. In addition, with

the positions of the first objective and the pinhole fixed, the spot size at the sample could be experimentally measured as a function of the micrometer position of the focus adjustment of the second objective. In this way, the spot size could be chosen by referring to a look-up table.

The modifications made to the spatial filter and collimator assembly and the addition of translation stages and the tilt table for aligning the assembly to the raw laser beam added significant weight to the system that wasn't present in the original design. It was discovered that the entire assembly must remain in place during the alignment or the additional weight would torque the system enough to throw the alignment off. The original alignment procedure called for the removal of the spatial filter and collimator assembly prior to starting the alignment of the scatterometer. The alignment procedure was therefore amended such that the spatial filter and collimator assembly would be bore sighted first and then placed on its supporting arm on the scatterometer prior to any other steps in the procedure. The spatial filter and collimator assembly could be translated out of the raw beam path so that the remainder of the original alignment procedures could be carried out as before.

### 3.2 New computer control subsystem

The original VAS was controlled from a FORTRAN language computer program running on a DEC PDP-11 minicomputer. The program controlled all functions of instrument control, data acquisition, data processing, 3-D data plotting, and data archiving. Plotting was accomplished with a 4-pen Hewlett-Packard plotter and data files were archived on large format tape cartridges. The computer controlled the various devices on the VAS through a digital interface composed of serial ports, parallel ports, analog-to-digital (A/D) inputs, digital-to-analog (D/A) control outputs, and IEEE-488 input/output (I/O). Devices controlled by the computer included an Aerotech stepping motor controller and indexer for the large rotary stage, a 3-axis stepping motor controller designed and built by Jim Grote and his assistants, the photometer gain

control, and the aforementioned plotter. In addition, signals were collected through the interface from the laser power monitor, the photometer, and a temperature/humidity probe.

The entire PDP-11 computer, computer peripherals, and digital interfaces were replaced with a new Zenith Z-248 personal computer. This computer contained an 80286-type, 8 MHz microprocessor with a 20 MByte hard disk, color monitor, and floppy drive. As archaic as this computer sounds at the time of this writing, it was more than adequate as a replacement for the PDP-11. It lacked the ultimate processor speed of the PDP-11, but it was much more cost effective than replacement of the aging PDP-11 and its failing peripherals, it took up less space, it would allow color data processing on its monitor, and could perform all the functions previously performed by the PDP-11.

Some new peripherals were also added to the Zenith computer. A Hewlett-Packard Model 7550 graphics plotter with an 8-pen cassette, an IEEE-488 interface, and an automatic paper feeder was added to accomplish data plotting. A MAXTOR Model PC800E Optical WORM drive with 800 MByte data cartridges was added for data archiving. At a later time, the Zenith computer was upgraded to a 12 MHz 286-type computer with a VGA monitor, a 40 MByte hard disk, and an IRWIN Model 445 tape drive with 40 MByte tapes. Still later, computer networking capability was added with the installation of a network adapter and the WORM drive was abandoned as the primary data archiving mass storage device. By the time the WORM drive needed maintenance, it was no longer a cost effective mass storage solution. In addition, if only raw binary data files were archived, data accumulated at a rate of less than 100 Mbytes per year, and archival could easily be satisfied by tape backup. This computer and peripheral configuration still exists at the time of this writing.

The Zenith computer was also fitted with an IEEE-488 interface bus adapter card for control of the various devices of the upgraded scatterometer. The original goal was to accomplish all interfacing through the IEEE-488 bus with the exception of reading the photometer signal

through the an A/D converter installed in the computer. This required that all the individual devices on the scatterometer conform to the IEEE-488 interface standard. Replacement equipment was added as described below. The A/D converter was initially used to acquire the signal from the photometer. At a later date, reading of the photometer signal was accomplished completely through the IEEE-488 bus as described below.

A major portion of the upgrade of the computer control subsystem involved development of an entirely new software control program. This was accomplished through the use of ASYST, a scientific data acquisition software package for personal computers. The ASYST software runs as a shell on top of the personal computer operating system and is coded through the use of word commands and groups of commands called colon definitions. Colon definitions are user defined words which accomplish a sequence of individual commands. The software also has the ability to swap in program sequences called transient overlays which allows the software developer to write a large and complex computer program while working within the computer's memory limitations. In this way, the program can be broken up into segments which are read into memory as needed and executed. The swapping of overlays is controlled by a main program which resides in memory as a permanent overlay.

A menu driven computer program was written to accomplish all of the data acquisition and data processing functions of the scatterometer. The program consists of a main program and nine transient overlays. The main program contains software routines which are required for all levels of scatterometer operation while the transient overlays are brought in to accomplish specific functions. Transient overlays are used for the following functions: 1) motor controller functions outside of the data acquisition loop, 2) changing and storing system parameters and scan parameters, 3) step-and-repeat data acquisition, 4) on-the-fly data acquisition, 5) calculation of data set statistics, 6) 2-D Cartesian coordinate data plotting, 7) 2-D polar coordinate data plotting, 8) 3-D data plotting, and 9) data conversion and miscellaneous data output.

The software program was essentially completed in early 1989 with improvements continuing for about a year. After that time, only minor bug fixes were accomplished and the software is still in use at the time of this writing. The software still does an adequate job of acquiring and processing the scatter data. However, much more sophisticated desk-top computers and data analysis programs now exist such that the data analysis functions of the scatterometer computer hardware and software are no longer efficient. While the data acquisition functions of the computer hardware and software are well matched to the rest of the system in terms of processor speed and memory, the 286 computer and the ASYST software package are essentially obsolete and therefore increasingly difficult to maintain. For these reasons, details of the software program will not be included in this report. A modern upgrade to the computer control subsystem would comprise a computer with a 386 or higher processor running a Microsoft Windows operating system and using a modern Windows-based data acquisition software package to provide the data acquisition function. Data analysis would take place on a separate, high performance, networked desktop computer with modern data analysis software.

### 3.3 New devices and interfaces

As discussed above, it was desired to create a data acquisition system that was connected via a single interface bus. Most of the instruments on the VAS were replaced with IEEE-488 compatible devices which could be connected to the computer via IEEE-488 compatible bus cables as discussed below.

#### 3.3.1 Motor controller

The two stepping motor controllers on the original VAS were replaced with a Klinger MC4/MD4 four-axis stepping motor driver and indexer system collectively referred to here as a motor controller. The new controller was compatible with the existing motors of the X, Y, and R

stages of the sample positioning subsystem, but not with the Aerotech rotary stage. The motor in this stage was replaced with a motor that could be driven with the Klinger controller. Commands are sent over the IEEE-488 bus which are then executed by the controller. In addition, the motor controller can report various aspects of the motors and the translation stages they drive, such as stage position and end of travel, and the controller can even store and run programs of stage motion sequences. Another advantage of the new motor controller is that it can control all four axes with common commands at a single IEEE-488 address.

### 3.3.2 Power monitor

The existing power monitor was replaced with a UDT Model S390 Multi-channel Optometer and a Model 228 HeNe laser detector. This unit has four separate channels which can be configured from the computer via the IEEE-488 interface bus at a single IEEE-488 address. The additional channels were included to allow easy addition of multiple laser sources operating at various wavelengths. In most cases, a single detector would not suffice for a wide range of wavelengths. The Optometer provides the most recent laser power reading for a given channel when requested by the computer. With only one channel active, the Optometer reads the laser power many times in the time it takes to move from one scatter data point to another. In addition, the Optometer can be set to integrate for various lengths of time.

In conjunction with this upgrade, the location of the detector was changed as discussed earlier in section 3.1.

### 3.3.3 Photometer

The original Photo Research Pritchard Photometer on the VAS could not be easily replaced with anything that was directly compatible with an IEEE-488 interface bus. The same type of photometer could be purchased with an IEEE-488 controller, but the response time was

too slow for the scatterometer system.

The original VAS had 3 different interfaces to the photometer control console: 1) an analog output voltage was read directly from the photometer's analog output jack through an A/D converter to get the scattered light signal; 2) a subset of the BCD output data lines were read to obtain the power of ten multiplier factor which the control console determines from a combination of the amplifier gain, aperture, and filter wheel settings; and 3) a set of TTL input data lines was used for computer control of the amplifier gain setting. This arrangement was employed in order to get the fastest step-and-repeat sample time. Computer control of the gain avoided the problem of gain change transients if the photometer was allowed to change the gain automatically. The voltage signal from the photometer takes a short time to settle down after a gain change, and readings of the voltage during the settling time are inaccurate.

In the original VAS, a reading of the scatter signal was made for each step of the stepping motors during a scan, even if the desired data interval was larger than a single step. In this way, the scatter signal would change slowly enough for the computer to anticipate when a gain change was needed. The computer would read the scatter signal at each point, determine if a gain change was needed, switch the gain setting if necessary, and continue. A complete BRDF measurement would be calculated and stored only at steps corresponding to the preset data interval. Later, this process was optimized such that the scatter signal was read at each multiple of two, three, or more steps to get the best trade off between data rate and data accuracy.

The efficiency of employing computer controlled gain is diminished, however, when the data interval is large. In the original VAS, the standard procedure for raster scans was to choose data intervals that were small compared to the laser beam spot size on the sample. With the trend toward larger sample sizes, e.g. semiconductor wafers, standard data intervals often were larger than the beam spot size. Under these circumstances, it was not desirable to employ computer control of the amplifier gain.

The problem associated with gain change transients can be handled in a different way. The BCD output of the photometer control console provides a data signal line called the "PRINT" indicator which indicates when it is appropriate to sample the remainder of the data lines. This line goes to logic level zero during a gain change. Experimentation demonstrated that monitoring this logic line was not a foolproof way of avoiding the gain change transients because the signal isn't completely settled when the line returns to logic level 1. However, there is clearly no reason to sample the data when the "PRINT" indicator is at logic level zero. In addition, there is a logic line called the "OVERLOAD" indicator which goes to logic level 1 when the digital readout of the photometer is overloaded, i.e., the reading is greater than 19.99. The readout often displays a momentary overload during a gain change, so this can also serve as an indication of when not to sample the data.

In addition to sampling the "PRINT" and "OVERLOAD" indicators, multiple readings of the photometer's analog signal can be made at each desired location on the sample and compared to one another until the readings reach a steady state. This solves the problem with transients and also provides a means of assuring a certain level of consistency in the data. It can also provide a diagnostic element in that the number of readings needed to reach a steady state value indicates the relative stability of the signal.

Using this new scheme of avoiding the gain change transients, it was no longer necessary to control the photometer gain. The photometer control console was set to "AutoRange" which means that the internal circuitry of the console adjusts the gain range of the amplifier circuit as appropriate. The photometer analog signal is sampled through the A/D converter in the computer as before. The power of ten multiplier factor is now read by connecting the data lines to a digital I/O converter made by IOTECH and identified by the model name "DIGITAL 488". This device converts the digital signals from the photometer BCD output to IEEE-488 compatible signals and resides as an IEEE-488 device on the bus.

A further development in this process was to abandon the reading of the scatter signal from the analog voltage output of the photometer and reading the signal from the BCD output instead. The photometer control console converts the analog voltage signal to BCD signals via an internal A/D converter and makes those signals available through the same BCD output connector where the power-of-ten multiplier factor is read. With this development, the entire photometer signal is now read via the IEEE-488 bus and the entire scatterometer now runs with a single computer interface.

The reason for abandoning the A/D converter as a means of sampling the scatter signal is that the speed of the A/D converter offered no real advantage. The speed at which the various devices on the IEEE-488 bus could be addressed was such that the step-and-repeat cycle time was long compared to the time it takes to sample the analog signal through the A/D converter. In fact, 100-1000 A/D readings can be averaged per cycle without significantly adding to the total cycle time. The computer code necessary to control the A/D board could also be abandoned, reducing the total size of the computer code.

As a final result of these changes, the step-and-repeat cycle time was slightly longer than the equivalent cycle time on the original VAS for small data intervals. However, the utility of the new system was greatly improved. Over a period of time, it became apparent that the comparison of two readings was more effective than monitoring the "PRINT" indicator, and that is the current practice at the time of this writing. The "OVERLOAD" indicator is used, however.

The step-and-repeat data sequence for the modified scatterometer is as follows: 1) the sample is translated to the desired location and orientation, 2) a programmable time delay occurs to allow the signal to settle, 3) the laser power meter is read, 4) the data string from the photometer is read, 5) the portion of the data string which contains the "OVERLOAD" bit is checked, 6) if the "OVERLOAD" bit is 1, the same delay time of Step 2 occurs, and program execution returns to Step 4; otherwise the process continues to the next step, 7) the bits in the

photometer data string are decoded to determine the reading and the multiplication factor, 8) another time delay occurs, 9) a second reading of the photometer is determined using Steps 4-7, 10) the two readings are compared, 11) if they differ by more than a preset percentage value, another reading of the photometer occurs until two sequential readings compare within the difference window, otherwise the process continues to the next step, 12) the BRDF is calculated using the final photometer reading, the laser power monitor reading, the current scatter angle, and the conversion factor. The sequence repeats by translation to the next desired location and orientation, all under computer control.

There is one variation on the preceding step-and-repeat sequence. If the photometer's reading is less than 1.99, the photometer is at its highest gain setting. This is because the value 1.99 is the changeover point for automatic gain changes. The photometer will continue to increase its gain in order to get the reading above 1.99 until it is at its maximum gain. Therefore, a reading below 1.99 indicates that the photometer is at its highest gain and is far from a gain change condition. For this reason, the process can be sped up by skipping steps 8-11.

In the preceding step-and-repeat sequence, the preset delay time and difference window are set by the operator in one of the program menus. The delay time is chosen to be longer than the update period of the photometer A/D converter. An update of the A/D converter occurs every 342 msec. The customary delay time has become 350 msec. In this way, it is assured that two consecutive readings from the photometer are read as opposed to two readings of the photometer occurring within a single update cycle of the photometer. The difference window is set such that the number of repeat readings and the uncertainty of the scatter measurements are minimized. However, these two conditions compete. If the difference window is too small, the normal fluctuations of the photometer reading will cause the software to cycle many times until two consecutive readings agree within the window value which ultimately slows down the measurement process. If the difference window is set too large, gain change transients may be

accepted as good readings and the uncertainty in the accepted measurements is too high.

### 3.3.4 Other

Finally, it should be noted that the measurement and recording of temperature and humidity with scattering data, as in the original VAS, was abandoned. At the time these modifications were made, the original temperature/humidity sensor was not functioning properly and no recent attempts had been made to correlate scatter data with temperature or humidity. Furthermore, the environmental conditions usually only fluctuated over a range of about 5° C in temperature and 10% in relative humidity. However, it should be further noted that some studies have shown the effects of temperature and humidity on the BRDF of certain samples<sup>7,8</sup> and therefore the environmental conditions should be controlled at the very least, and preferably tracked in some way, when making scatter measurements.

#### 4. NEW SCATTEROMETER CAPABILITIES

Following the modernization and improvements discussed in the previous section, several new capabilities were designed and/or added to the scatterometer which were not part of the original VAS, either in form or function. Two such capabilities which were realized included rudimentary linear polarization control of the incident laser beam and the ability to scan a sample up to four inches across. In addition, initial work was accomplished in adding multiwavelength capability to the scatterometer and some designs were conceived for increasing the number of motor-driven, computer-controlled, translational degrees of freedom for alignment and sample manipulation.

##### 4.1 Polarization control

Polarization control was accomplished by adding a Newport Model PR-550 broadband, visible wavelength, polarization rotator between the upper and lower mirrors of the existing Newport Model 675 beam steering instrument. The polarization rotator was mounted via a threaded plastic adapter mounted to a two-axis pitch and yaw tilt stage which in turn was mounted to an aluminum bracket which in turn was mounted to an additional Newport Model 375 rack and pinion rider and clamp. The plastic adapter and the aluminum mount were machined in house. The Model 375 is the same part used to mount and translate the mirrors of the beam steering device.

The polarization rotator is used to rotate the linear polarization state of the laser beam with 98% transmission for visible wavelengths. This gives the scatterometer the flexibility of making scatter measurements as a function of incident polarization state of the laser beam. The degree of linear polarization of the beam, when incident on the sample plane, is not as high as when it exits the laser because the beam reflects off of two mirrors which have a rather large

effect on the linear polarization state of the beam. The scatterometer has a linearly polarized HeNe laser incorporating a Brewster window. The polarization ratio, here defined as the ratio of the maximum to minimum power through a linear polarizer,  $P_{\max}/P_{\min}$ , is approximately 1600 just after the beamsplitter in its new location. The polarization ratio of the beam incident on the sample, without the polarization rotator in place, is approximately 124 and is therefore elliptical in its polarization state.

The choice of location for the polarization rotator was dictated by the size of the rotator. For polarization control, it is perhaps the worst choice. With the polarization rotator in place and adjusted to produce maximum power in the s-polarization state at the sample plane, the polarization ratio, as defined before, is approximately 97. With the rotator adjusted for maximum power in the p-polarization state at the sample plane, the polarization ratio is approximately 47. The polarization ratio can be evened out somewhat by placing a linear polarizer just prior to the polarization rotator.

A better solution for polarization control would be to use a smaller polarization rotator, mount it after the last turning mirror of the beam steering instrument, and place a high quality linear polarizer between the rotator and the last turning mirror. This would lower the total power incident on the sample plane and may require a more powerful laser. An unpolarized laser may also be appropriate.

In general practice, the polarization rotator is not used. The laser itself has been rotated such that the aforementioned elliptical polarization state of the incident beam, with its polarization ratio of 124 at the sample plane, is oriented with the major axis of the ellipse at  $45^\circ$  to the plane of incidence of the laser beam. In this way, the incident polarization is mixed as much as possible between s and p polarization.

#### 4.2 Four-inch sample translation

The original Klinger x- and y-axis translation stages, capable of 25 mm of travel, were replaced with Klinger model UT100.100 stepping motor driven translation stages capable of 100 mm of travel and incorporating center origin search and rotary encoders. In order to accommodate the additional load of the larger translation stages, the existing Klinger rotation stage was replaced with the larger Klinger model RT-200 stepping motor driven rotation stage with origin search and rotary encoder.

The origin search feature moves each stage to an origin location with a single command to the motor controller. The software can send all three stages to their respective origins in sequence with a single keystroke at the computer keyboard. This saves several initialization steps which previously had to be accomplished every time the scatterometer was turned on. This previous procedure was referred to as zeroing the stepping motors. The large rotary stage is still zeroed in the original manner by moving the stage until the laser beam, reflecting off the sample, hits the photometer's lens cap target.

The rotary encoders on the new stages can be used to give feedback on actual rotation of the stepping motor regardless of how many voltage pulses were sent to the motor. In other words, the encoder can verify that the stepping motor rotated one step for each step sent by the controller.

The total load of the larger translation and rotary stages put additional torque on the cradle and its support structure. The torque was compensated by adding two adjustable feet at the rear of the cradle. The feet can be adjusted so that alignment is maintained for various positions of the large linear translation stage for sample thickness adjustments, and the rotary stage for changes in incident angle of the laser. In addition, the increased length of the x- and y-axis translation stages required the R-axis to be raised 0.25" and a slot to be machined out of the cradle to allow clearance for the X-axis translation stage motor during sample rotation when at

extremes of Y-axis travel. Raising the R-axis in turn required the photometer to be raised by the same amount since the R-axis and photometer axis need to be aligned with each other for proper system alignment. The cover of the optical table was raised by about 9 mm with the insertion of Plexiglas shims. This new height of the optical table cover allowed a clearance of about 0.15" for the X-axis translation stage motor during sample rotation when at extremes of Y-axis travel.

The modifications which had to be made to accommodate the additional size and mass of the new stages exemplified one of the primary limitations of manipulating samples held vertically. The increased mass puts enormous demands on the support structure, and mechanical alignment stability is often poor. Each successive increase in linear translation capability requires a larger rotation stage to handle the increased load which in turn adds additional mass to the support structure. In addition, any further increase in x- and y-axis translation capability would require another increase in the optical axis elevations which would put the R-axis higher on the support structure, further aggravating an already difficult mechanical stability problem. For these reasons, any increase in sample size capability is not recommended for the scatterometer in its present vertical sample configuration. This limitation was a major driver for designing a scatterometer which manipulates samples horizontally, as described in Section V.

#### 4.3 New photometer

A new Pritchard aperture photometer, model PR-1980A made by Photo Research, was added to the scatterometer. This replacement is the same model as was on the original VAS, but slightly updated and containing some options not incorporated in the older model. The new model contains a thermoelectric cooler for the photomultiplier tube (PMT) which gives a more stable signal, especially at higher gain settings, and a higher sensitivity by about a factor of two. The cooler keeps the PMT at about 5° C. In addition, three narrow bandpass filters were installed in the rear filter wheel of the photometer corresponding to three primary wavelengths of a

proposed multiwavelength scatterometer. The previous photometer had a single narrow band filter centered at 632.8 nm. The new photometer has narrow bandpass filters centered at 441.6, 543.5, and 632.8 nm corresponding to the laser wavelengths of HeCd (blue), HeNe (green), and HeNe (red), respectively.

There are three additional differences between the new photometer and the previous one. The new photometer does not have the circuitry necessary for computer control of the gain settings. Since computer control of the gain has been abandoned, this poses no problem. In addition, the new photometer does not have the wide band signal output feature which can be used to get the fastest response from the PMT. This feature was never used on the previous photometer. Finally, the thermoelectric cooler on the new photometer requires periodic changes of desiccant capsules used to absorb any moisture which might otherwise condense on the cold PMT. The signal stability, as displayed on the photometer's digital panel meter, fluctuates more as the humidity near the PMT increases. This serves as an approximate gauge of when to change the desiccant capsules. The recommended replacement interval for lower humidity environments is about every six months.

#### 4.4 New laser sources

Two new laser sources were procured for a proposed multiwavelength scattering capability. A nominal 17 mW, 441.6 nm HeCd laser and a 0.5 mW, 543.5 nm HeNe laser, together with the existing 632.8 nm HeNe laser, would provide three wavelengths spanning the visible spectrum at roughly 100 nm intervals. The HeCd laser could not be easily incorporated onto the main rotating scatterometer platform because of its size, so laser beam delivery systems were procured which would deliver collimated laser light to the platform. The laser beam delivery systems are single mode optical fibers with custom beam coupling optics attached on both ends. These systems offer relatively easy input coupling for collimated laser beams and they produce

collimated output with a specified beam diameter.

Addition of the new laser sources to the scatterometer has not been accomplished at the time of this writing for several reasons. The utility of the scatterometer, even with its single wavelength, has kept it in fairly constant demand. The additional capability afforded by multiple laser sources has not, as of yet, outweighed the down time associated with conversion to a multiwavelength scatterometer. In addition, the requirement to make scattering measurements at UV wavelengths has recently become more important. Conversion to UV wavelengths would require a change in the photometer and would also require visible wavelength alignment beams. If the conversion to UV wavelengths occurs, adding additional visible wavelengths would be relatively easy to accomplish at the same time.

#### 4.5 Additional motor-driven translations

The current scatterometer has several manual translation and rotary stages which require adjustment for alignment purposes and for setting up the scatterometer for a sample run. Motorizing these stages and applying remote controls could greatly improve the automation of the instrument, increase repeatability in sample mounting and alignment, and reduce some of the tediousness of system alignment. Although no equipment has been procured to effect any such modifications, the additions would be straightforward and relatively uncomplicated.

There are two stages on the main rotating platform of the scatterometer which could be motorized. The large linear translation stage, which is used to place the sample surface being measured at the intersection of the R-axis and the laser beam, allows adjustments for differences in sample thickness and for differences in sample holders which are mounted to the sample positioning subsystem. Making these adjustments requires two people, one to look through the photometer to see when the beam spot is under the Pritchard aperture while the other person adjusts the stage, or a single person to make repeated adjustments, moving back and forth

between the stage and the photometer. This procedure also relies on the operator's judgment in determining when the beam spot is centered under the Pritchard aperture. In addition, the brightness of the beam spot is often too low to perform this operation with high repeatability.

A solution to this problem would be a motorized translation stage controlled in a similar manner as the other computer controlled stages. The stage could be controlled via computer keyboard commands while the operator looks through the photometer eyepiece, or the computer could find the appropriate position by reading the photometer output and moving the stage until the reading is maximized. The maximum photometer output in most cases will coincide with the beam spot being centered under the Pritchard aperture.

The second manual stage on the main rotating platform of the scatterometer is the rotary stage used to change the angle of incidence of the laser beam. Although the angle of incidence is easy to change during normal operation, certain alignment procedures are best performed by repeated back and forth rotations of this stage. Here again, it takes two people to perform this operation. A motor driven stage would allow one person to perform this operation and some portions of the alignment could also be automated further by programming the computer to find the best alignment.

The remainder of the manual adjustments are all part of the laser beam positioning and conditioning subsystem. In this subsystem, there are 10 translation, 3 rotation, and 4 tilt degrees of freedom with an additional two tilts when the polarization rotator is in place. Many of these are rarely adjusted during normal operation, but several require tedious adjustment during system alignment and therefore are good candidates for automation. Future design work in this area is being considered.

## 5. NEW SCATTEROMETER DESIGN

When the scatterometer was upgraded with 4-inch linear translation stages and a larger R-axis rotary stage, it became apparent that the vertical sample mounting orientation had reached a practical limit. The length of the 4-inch linear translation stages could just barely be accommodated by machining a slot into the cradle onto which the sample mount and sample translation system are attached. This slot allowed the x-axis translation stage to rotate when the sample was displaced to the maximum travel of the y-axis translator. In addition, the mass of the larger R-axis rotary stage, which was necessary to handle the increased load of the 4-inch linear translation stages, and the mass of the linear translation stages themselves, caused increased mounting torque on the cradle and the linear translation stage to which the cradle was mounted. These torques in turn made it more difficult to align the R-axis tilts, caused a decrease in the alignment stability due to mechanical creep, and required additional supporting feet at the rear of the cradle. Even with the large increase in capability provided by the 4-inch translators, it was recognized that it would only be a matter of a few years before samples larger than 4 inches would be common, given the rapid growth of semiconductor wafer diameters.

With the above issues in mind, a new scatterometer design was conceived to overcome the sample size limitations and mechanical problems of the vertical sample orientation. The following discussion describes the design, which should be better suited for semiconductor materials research.

The new design differs primarily in the way the sample is manipulated under the incident beam. Instead of mounting samples vertically and having the incident laser beam and the detector in a horizontal plane, the sample is held horizontally while the laser beam is incident in a vertical plane. Because of the nature of the detector, which is a large photometer with an integrated viewing system, the scattered light is folded into a horizontal plane so that the detection is still

horizontal. This design should give a more stable sample manipulator with a much smaller overall footprint than the existing scatterometer

The following is a description of the scatterometer design in reference to the figures shown at the end of this section.

Fig. 1 shows a front view of the sample manipulator whose purpose is to provide translation and rotation control of the sample under the incident beam. It consists of a sample mount to hold a sample, such as a semiconductor wafer, by either a mechanical or a vacuum suction means. This is mounted on top of a linear translation stage (x-axis) which in turn is mounted on another linear translation stage (y-axis) which is mounted on a rotation stage (r-axis) which is mounted on a vertical translation stage (z-axis) which is mounted to an optical table. The x, y, and r axes provide measurement degrees of freedom for manipulating the sample under the incident laser beam (not shown in this figure). The z-axis translator is for sample alignment in order to accommodate samples of different thickness. The spacer between the y and r axes allows the x and y motor cables to be conveniently placed. The x, y, and r stages are computer controlled and driven by stepping motors. The z stage is manually operated.

Fig. 2 is a side view of the fiber manipulator whose purpose is to precisely align the incident laser beam and control its angle of incidence. The fiber manipulator consists of an arm (inset) which holds the output ends of fiber collimator assemblies side by side in a line. The present design calls for 3 such fiber collimator assemblies carrying the output of three separate lasers. The output of each fiber collimator points downward toward the sample. Only one fiber emits a beam at any given time. The arm sits atop two translation stages followed by two goniometers. These four stages provide pointing and positioning of the laser beams such that the beams can be aligned to the axis of rotation of the r-axis stage of Fig. 1. These four stages are manually adjustable. This entire assembly is mounted to a stepping-motor-driven goniometer stage capable of changing the angle of incidence while keeping the chosen laser beam pointed at

the intersection of the r-axis rotation stage and the sample surface. The final linear translation stage allows the entire fiber manipulator to be translated since only one beam can be properly positioned at any given time.

Fig. 3 shows a front view of the fiber manipulator, again with the full arm shown as an inset. The goniometer stage, now seen in profile, provides rotation about a point in space coinciding with the intersection of the r-axis and the sample surface.

Fig. 4 shows a side view of the sample and fiber manipulators together in their proper relative positions. Not shown here is a mirror assembly situated directly above the sample manipulator and above the elevation of the fiber arm. The mirror directs the scattered light toward a Pritchard aperture photometer which is mounted in a horizontal direction looking toward the mirror assembly. From the figures, it is obvious that the photometer will not see the sample surface for a laser beam angle of incidence normal to the sample. The goniometer needs to be positioned so that the angle of incidence is to either side of the normal, which is the usual case for light scattering measurements.

The remainder of the design is similar to the present system as far as laser power monitors, motor controllers, photometer controller, interfaces, computer, and peripherals are concerned. Not shown in the above four figures are the fiber couplers and beamsplitters for coupling laser light into the fiber cables and for monitoring the lasers' power.

This design is complete in itself, but offers one less degree of freedom than the present system offers since there is no means of changing the scattering angle. All measurements would be carried out with a scatter angle of  $0^\circ$  which is the scatter angle routinely used in this laboratory to make raster scan measurements of semiconductor wafers. The additional degree of freedom could be added through the use of another goniometer stage, however its absence does not cause significant difficulties or disadvantages for the intended purpose of this new design.

Most of the parts for building a scatterometer to this design were procured under this

work unit and partial assembly and testing was completed. At the time of this writing, the need to measure 150 mm GaAs wafers has recently arisen. Completing the assembly is the only short term solution to providing light scattering measurements of the entire surface area of 150 mm wafers.

# New Scatterometer Design

## Sample Manipulator

### Front View

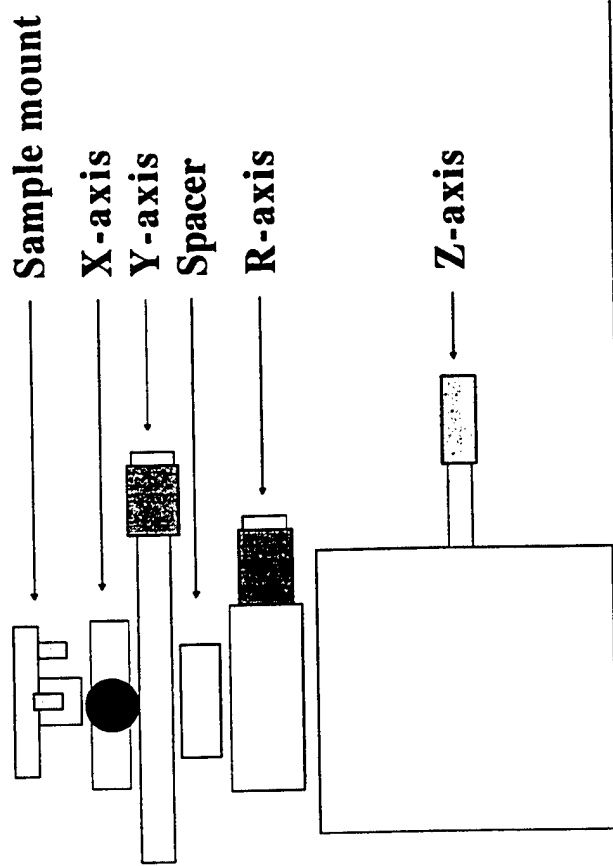


**Fig. 1.** Front view of the sample manipulator.

# New Scatterometer Design

## Fiber Manipulator

### Side View

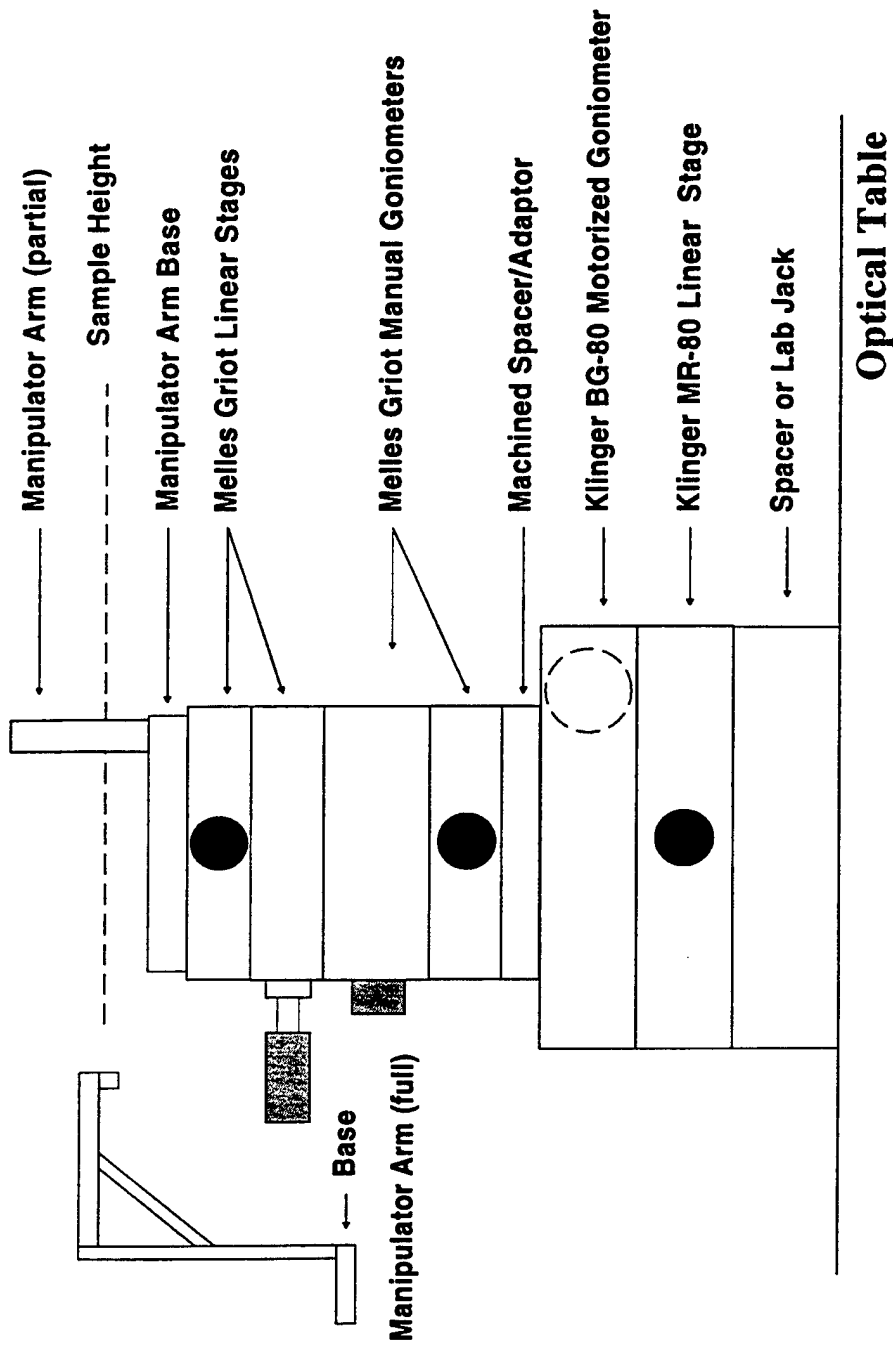
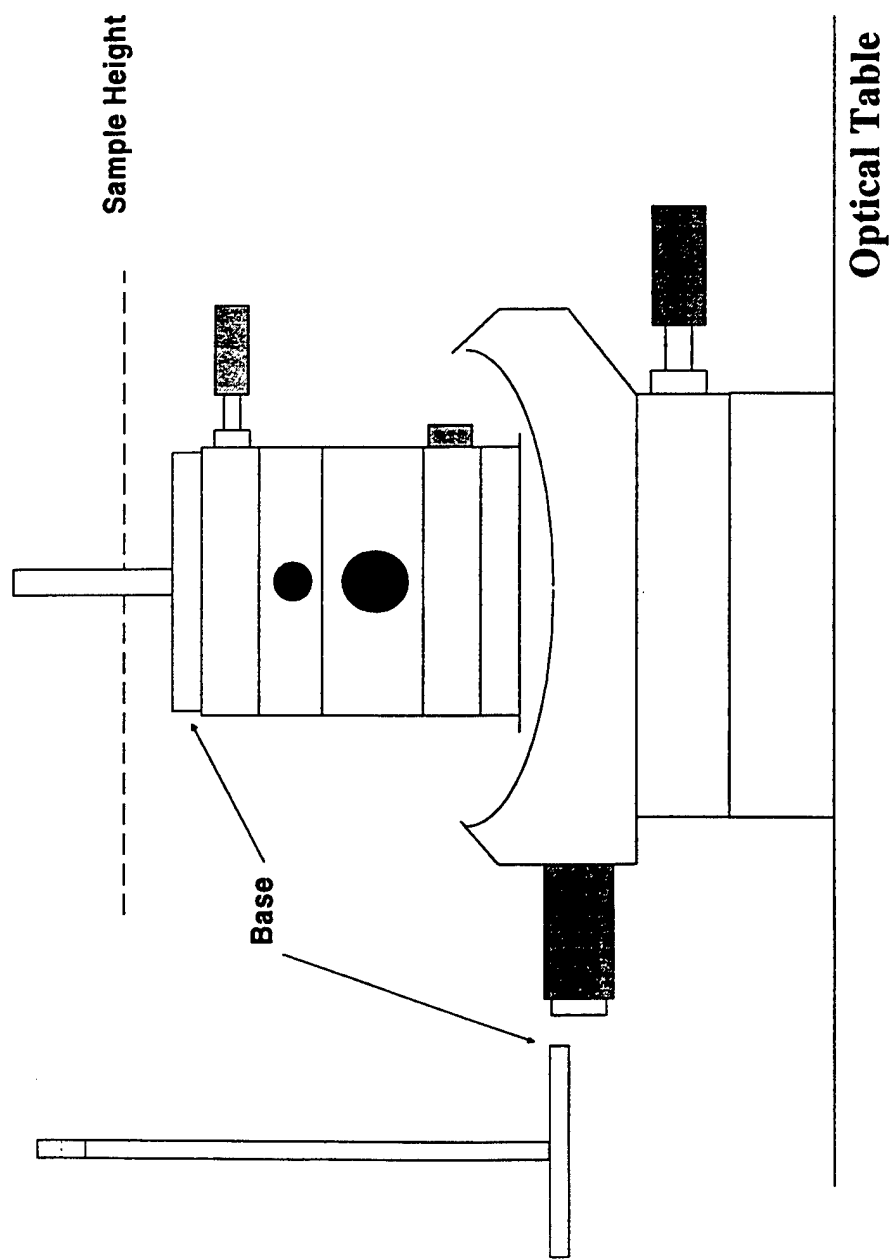


Fig. 2. Side view of the fiber manipulator.

**New Scatterometer Design**  
**Fiber Manipulator**  
**Front View**



**Fig. 3.** Front view of the fiber manipulator.

# New Scatterometer Design

## Side View

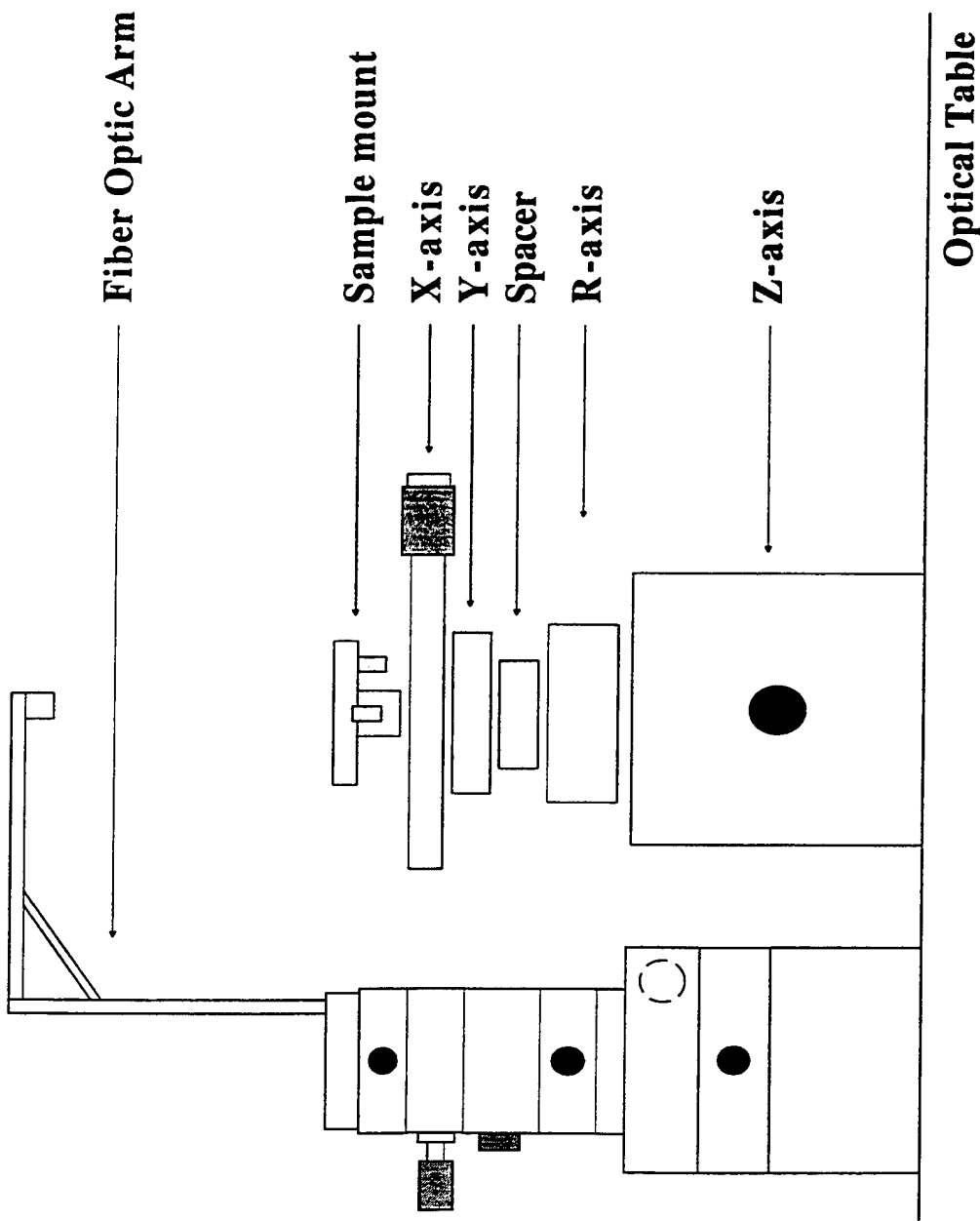


Fig. 4. Side view of the sample manipulator and fiber manipulator.

## 6. SUBSURFACE SCATTER STUDIES

One of the reasons for pursuing a multiwavelength scatterometer is to study subsurface scatter. Subsurface scatter is scatter that originates in the region just below the surface, but is distinguished from bulk scatter in that subsurface scatter is generally attributed to subsurface damage from cutting, grinding, and polishing of a material. A material may be topographically smooth but still scatter light if the light can penetrate the surface and scatter off inhomogeneities near the surface. Various polishing flaws and the overall polishing quality and uniformity are the major sources of surface scatter in state-of-the-art optical and semiconductor materials, so it is important to understand the subsurface scatter contribution as well.

Stowell, et al., compared the BRDF from both sides of the front surface of transparent samples and found a significant difference.<sup>8</sup> This is accomplished by making a raster scan of a sample in the usual way, then flipping the sample over in its holder and measuring the scatter with the laser incident on the same area, but from the back side of the sample. The BRDF from the back side of the front surface was greater than the BRDF from the front side of the front surface for the samples reported, while identifiable features in both scans clearly showed that the same area was scanned in both cases. This result is interesting because it allows some insight into the physical nature of the material near the surface of a polished sample and, therefore, transparent materials can serve as models for nontransparent surfaces. However, the results by Stowell, et al., were never clearly explained in terms of the optical properties of material near the surface.

Many materials, like Si and GaAs, are not transparent to visible wavelengths. In order to determine the relative contribution of subsurface scatter to the total BRDF, two approaches are proposed here:

- 1) Make scattering measurements at several wavelengths and take advantage of the differences in penetration depth of the light at the different wavelengths as a means of depth

profiling. Presumably, measurements made at wavelengths with the lowest penetration depth would have the least amount of subsurface scatter contribution while wavelengths with the greatest penetration depth would have the largest, although absorption factors would have to be taken into account.

2) Measure the topography of a surface by atomic force microscopy (AFM) and calculate the scatter for a clean, smooth, front-surface reflector with the same topography based on Rayleigh-Rice perturbation theory.<sup>9</sup> Presumably, any measured scatter in excess of the theoretical surface scatter would be nontopographic scatter and could be attributed to subsurface scatter.

Neither of these approaches has been completed although much of the instrumentation is available and it is still a goal in ongoing surface characterization work. Recent work has indicated that topographical imperfections, in the form of residual polishing scratches and not subsurface damage, are responsible for a large proportion of scatter measured from certain GaAs wafers. However, it is still not clear what the relative contributions to the total BRDF are from surface (topographical) scatter and subsurface (polishing damage) scatter.

Another reason for pursuing multiwavelength scatterometry is to be able to explore wavelength scaling. Wavelength scaling is the ability to mathematically relate scattering at different wavelengths.<sup>10</sup> Different materials wavelength scale to varying degrees and therefore wavelength scaling is a property of the material. If it is known that a material wavelength scales, then scatter measurements need only be made at a single wavelength and scatter can be calculated for other wavelengths. However, in order to determine if a sample wavelength scales, a multiple wavelength scatterometer is required.

To a certain extent, wavelength scaling is related to the issue of subsurface scatter because the existence of subsurface scatter for an otherwise smooth and clean surface would be a primary reason for failure to wavelength scale.

## 7. BRDF ROUND ROBIN

In early 1988, the scatterometer system was included in a national BRDF Round Robin. At that time, none of the modifications previously described in this report had been implemented and so the instrument was essentially the original VAS. The results were excellent in comparison to other scatterometers and some deficiencies in the VAS were realized which were subsequently corrected as described below.

The round robin was part of a study of BRDF measurements for the Microtopography and Contamination Programs at Rome Air Development Center (RADC). The goal was to survey the capabilities of the scatter measurement community and to gather a database for the Air Force to evaluate the usefulness of BRDF measurements. Eighteen laboratories from industry, government, and academia measured samples from a standard set of four. These four samples had varying degrees of scatter from diffuse to specular. The results were published in a paper by Leonard and Pantoliano,<sup>11</sup> and the data from the VAS is designated as Laboratory #7 in this report. Dr. Leonard visited most of the facilities in the study to ensure measurement consistency and this was the case here.

The four samples in the round robin measurement set consisted of a diffuse white-painted Al disk which had Lambertian characteristics with a reflectivity of approximately 0.86, a diffuse black-painted Al disk, a Mo mirror, and an Al mirror. All the samples were 2" in diameter. The BRDF of these samples covered a range of approximately 5 orders of magnitude.

BRDF angle scans were performed at five locations on each sample - those being on center and at the four corners of a square of area 1 square cm about the center. For the measurements made with the VAS, the beam had a spot size of approximately 1.0 mm in diameter and was nominally s-polarized with an angle of incidence of 10°. The 20' aperture on the photometer was used. The angle scans were made from 0° (normal to the sample) out to 70° for

the nonspecular samples and from 15° to 70° for the specular samples. The scale factor for conversion to BRDF units was determined using the 20' aperture on the photometer and the barium sulfate plaque as the Lambertian reference.

The results of the round robin show that, out of the 10 laboratories that measured all four samples, the measurements made on the VAS had the lowest average absolute deviation from the mean for the four samples, using the data tabulated in the reference (see Table 1 of the reference).<sup>11</sup> All of the plotted data in the reported work show the VAS data to be in the middle of the pack for all angles and all samples. Even though there were problems encountered during the measurements as discussed below, the results indicate that the VAS was capable of measuring BRDF with more reliability over a wide range of samples and scatter levels than any other scatterometer in the study.

Several problems were encountered during the round robin measurements. The first one involved alignment of the barium sulfate reference material. In order to convert the raw data from the scatterometer into BRDF units of inverse steradians, a scale factor is determined by measuring a Lambertian reference material. The theoretical BRDF for a Lambertian material is  $\rho/\pi$  for all scattering angles where  $\rho$  is the total hemispherical reflectance of the material. By measuring a Lambertian material with the scatterometer, a scale factor can be calculated that incorporates all of the fixed parameters in Eq. 1. These include the solid angle  $\Omega$ , the proportionality constant between the photometer signal and the scattered power, and the proportionality constant between the laser power monitor signal and the incident power.

The problem with using a diffuse scatterer like barium sulfate is that it is difficult to align the surface parallel to the translation plane of the (x,y) translators which is the same thing as saying perpendicular to the photometer axis and the R-axis. If this condition isn't met, then translating the diffuse surface will cause the beam spot on the sample to move off the intersection between the surface and the photometer axis, to the point that some or all of the beam spot is

outside of the Pritchard aperture spot. This in turn would lead to a less than desirable reference measurement. Since Lambertian materials like barium sulfate are not necessarily perfectly homogeneous across a given surface area, it is customary to measure many points on the surface of the reference material when making a reference scan. The problem discussed here is especially acute when using the smallest aperture, the 2' aperture. It should be noted that alignment of specular samples is accomplished by spinning the sample about the R-axis and adjusting the sample tilt until the reflected beam spot no longer traces out a circular pattern, but remains stationary in its pointing direction. This is also a step in the system alignment procedure prior to aligning the various axes with respect to one another.

The solution to this particular problem during the round robin measurements was to use the 20' aperture. There is, however, a better solution for general practice which was worked out after the problem was discovered. By simply translating the sample from one extreme of its surface area to the other, the amount of relative motion between the beam spot and the aperture spot can be determined. By the use of a simple visual model of a plane, representing the sample surface, and two lines intersecting the plane, the first being the photometer axis and the second the laser beam, one can determine which way the surface is tilted from being perpendicular to the photometer axis. An adjustment to the sample tilt stage can be made and the process repeated until, after a few iterations, the beam spot no longer strays outside of the aperture spot for even the smallest of the Pritchard apertures, the 2' aperture. This solution is now common practice for alignment of all diffuse samples.

The discovery of the diffuse sample alignment problem begs the question of how reliable previous reference measurements were. It is unknown to the author whether or not this problem had been recognized previously and only rediscovered at the time of the round robin. There is no reference to this issue in the original VAS report, nor is there any reference to a recommended aperture setting for the measurement of diffuse samples. It turns out that only large misalignment

tilts have a correspondingly large effect on the outcome of the calculated scale factor; but since reference scan data was not routinely archived, it is impossible to review past reference measurements to see if there was an alignment bias. Having stated this, it is still quite important to have a procedure for aligning diffuse samples to avoid serious blunders.

A second problem encountered in the round robin was that the VAS software was written to calculate BRDF without the  $\cos\theta_s$  term of Eq. 1. This came to light when measuring the diffuse white sample in the round robin measurement set. For a Lambertian surface, an angle scan should give a flat response if using Eq. 1 because the scattered intensity from a Lambertian surface falls off as  $\cos\theta_s$ . For the round robin, the solution was simply to divide the results of the measurements by  $\cos\theta_s$ .

The fact that the software calculated BRDF without the  $\cos\theta_s$  term was, to some extent, a matter of choice. At the time the software was written, there was some disagreement as to the most practical definition of BRDF for experimental measurements. Both definitions can be found in the literature.<sup>3</sup> In the new software described in Section III, the more standard definition stated in Eq. 1 was used.

Another aspect of the scatterometer which was highlighted during the round robin was that the aperture settings on the photometer are not aperture stops. Typically, scatterometers are built with multiple aperture stops. The larger stops are used in order to get good signal to noise ratios for low scatter measurement away from the specular direction, and smaller stops for near-specular measurements. Calculating BRDF in this case requires that the appropriate value for  $\Omega_s$  be used, which corresponds to the solid angle subtended by the aperture stop used to make the measurement. However, in the Pritchard aperture photometer, the apertures are field stops.

The Pritchard aperture photometer is essentially a radiance meter. The apertures are chosen such that each increase in aperture size represents an order of magnitude increase in the area imaged onto the PMT for a given distance. It is calibrated in such a way that if an extended

light source of uniform radiance is measured, the response of the photometer, i.e., the radiance measured, will be the same regardless of the aperture size so long as the extended source is larger than the field of view afforded by the aperture. The photometer circuitry automatically accounts for this increase in field of view. For this photometer, the solid angle  $\Omega$ , in the BRDF calculation is fixed by the size of the input lens, a 7" focal length, f3.5 lens.

In light scattering measurements, it is best to use a field of view which is larger than the extent of the laser beam spot on the surface. If this is always the case, then changing the aperture setting on the photometer does not change the amount of light collected, as in a typical radiance measurement. As a result, the BRDF measurement would change by one order of magnitude for each change in the aperture setting without a new reference scan and a newly calculated scale factor

This hadn't been a problem in the past because the standard practice was to use the smallest aperture setting on the photometer for all measurements. However, when comparing scatterometer instruments, measurement practices, and results, it is important to know the exact function of each optical element in the instrument.

The final problem encountered in the round robin measurements was a stray light problem encountered at high scatter angles. The initial angle scans on the specular samples increased at high scatter angles after the usual falloff. This indicated that stray light was getting to the detector, possibly via a specular reflection off the sample. This was remedied by repeating the measurements in the dark.

Standard practice has always been to make scatter measurements with the lights on because the photometer contains a narrow band filter which only allows light in a narrow range of wavelengths to pass through to the PMT. In general, this is acceptable practice because the possible conditions under which significant stray light of the proper wavelength can get to the PMT are rare. A common scenario is to measure scatter only at normal incidence from very low

scatter surfaces. For this scenario, there is no specular route for light from any light source to get to the detector. Only diffuse light illuminating the sample can be scattered toward the detector. Since the diffuse ambient light in a narrow band centered at 632.8 nm and incident on the area of the sample seen by the PMT is quite small, and since only a tiny fraction of that is scattered toward the PMT for ordinary low scatter samples, ambient light is not a concern. In fact, measurements made in the dark under these conditions are identical to measurements made with the lights on within measurement uncertainties.

This is not the case, however, for nonzero scatter angles. Diffuse light scattered from bright objects in the room, primarily the walls, has a direct specular route to the PMT if a highly reflective sample is being measured. Any light source in the measurement plane of the scatterometer could have a specular route to the PMT at certain scatter angles, but there never has been a light source at this level in the scatterometer lab.

The source of the stray light in the round robin case was never conclusively determined. Several times, in subsequent measurements, system checks were performed to determine the difference between measurements made with the lights on and off. Little difference was ever found for most of the measurement scenarios, indicating that stray light is not usually a problem. One possible source of the stray light in the round robin measurements could have been the lights from a clean bench behind the scatterometer. The lights were approximately 2 ft above the measurement plane of the scatterometer, so there was no specular path. However, they were situated in such a way that they could illuminate the sample at the scatter angles where the anomalous increase in scatter was observed. This means that the samples would have to have scattered enough light into the measurement plane to affect the BRDF scan. It was never clear whether or not this could account for the increase.

## 8. GALLIUM ARSENIDE MATERIAL MEASUREMENTS

At the beginning of this work unit, the focus of scatterometer measurements was on ring laser gyroscope mirrors, glass substrates for mirrors, and optical components in general, where the amount of surface scatter was related to optical performance of the sample being tested. In mid 1988, a shift began toward measurement of GaAs and related semiconductor materials. For these materials, the emphasis is not on how they perform as optical elements, but rather how they perform as semiconductor device substrates. In both cases, the quality and uniformity of the polish are the issue, but in the latter case, the polish becomes a factor in the processing of useful solid state devices, and scatter measurements can be used to quantify uniformity and compare different polishing processes since the scatter should be dominated by polish related imperfections. Correlations between raster maps of the surfaces and other material and device parameters were sought. At the same time, the relationships between scatter and the physical nature of the material, such as surface roughness and subsurface damage, were to become an active research effort.

Since state-of-the-art semiconductor substrates, such as Si and GaAs, are not transparent to visible wavelengths and are highly specular, scatter measurements are made in the same way as for mirrors. The only major adaptation was the construction of sample holders for the thin, large diameter wafers. Two-inch diameter wafers could be accommodated by simply installing a plug in the standard 2" optic holder, to take up the depth of the holder, and a threaded ring to contact the edge of the wafer. However, at the time these early measurements on semiconductor material began, the scatterometer still only had 1" translation stages. Requirements called for full wafer analysis to within 2 mm of the wafer edge.

The requirement for full wafer mapping was the major impetus for adding 4" translation stages to the scatterometer as discussed in Section IV. However, prior to this modification, 1"

square areas at the center of 2" wafers were scanned in the early phases of GaAs measurement. Soon after, a translation adapter was constructed which allowed a 3" wafer to be offset with respect to the one-inch translation coordinate system. The adapter allowed a 3" wafer to be scanned with nine individual 1" square scans by offsetting the wafer holder +/- one inch in both x and y. The data was subsequently pieced together with software on a separate computer system. This effort was required because full wafer data was to be correlated with other data taken over entire wafers. Few wafers were ever measured this way, but it did constitute a proof of concept and did provide an early opportunity to insert scattering data into measurement correlations for GaAs material programs. This tedious task of measuring and piecing together data was no longer necessary when the (x,y) translators were upgraded to 4" travel.

The early efforts at GaAs light scattering were made on substrates which were either part of the program entitled "Manufacturing Technology for Solid-State Microwave Systems" or they were from SBIR or other miscellaneous programs. Approximately five 3" wafers were characterized through early 1989.

A much larger effort was expended on MIMIC Phase 1, Task 4.e, "Materials/Device Correlation Program. During the time period of May 1989 through Apr 1991, approximately 85 GaAs wafers were measured and the data supplied to the program database. Of these 85 wafers, about 75 were 3" diameter and 10 were 2" diameter wafers. In addition, some early work was performed in evaluating 3" wafers with epitaxial layers. These wafers represented a cross-section of substrates being processed by contractors in the MIMIC program and they came from several sources. In addition, the single crystal boules from which the wafers were sliced had been grown by several methods. Details of the polishing processes for these wafers was never obtained.

One clear result of the work on Task 4.e was the existence of a scattering signature for wafers coming from a particular manufacturing source. The two primary factors in the scattering signatures of these GaAs wafers was the median BRDF for an entire raster scan of the surface and

the degree to which that scatter was homogenous with respect to rotation of the wafer. This signature was so repeatable that the number of measurement scans and the total measurement time necessary to characterize a particular wafer could be predicted simply by knowing the source of the wafer. The implication here is that each manufacturer has a polishing process that produces unique residual polishing features which in turn produce unique scattering signatures. The scattering signatures have also carried over to 4" diameter wafers as determined by more recent measurements.

In the process of analyzing the large number of wafers in the Task 4.e program, a standard procedure was developed for measuring large wafer substrates. A paper describing this procedure and some of the aspects of the scatter variations seen on GaAs wafers from the various manufacturers was presented soon after the Task 4.e work was concluded.<sup>12</sup>

A follow-on program to MIMIC Phase 1 contained an effort to continue looking at GaAs materials issues, although scaled back in the materials characterization area. This program, the MIMIC Phase 2 Test Structure Wafer Analysis Program, resulted in a somewhat steady flow of mostly 3" GaAs wafers requiring similar characterization as that provided in Task 4.e for the purposes of tracking any changes in the properties of GaAs wafers being used by contractors in the Phase 2 program. Wafers measured for this program provided further verification of the previous Task 4.e results and the data files are archived in what might be the largest light scattering database on GaAs wafers in the world.

Another effort in materials characterization, which began near the end of the this work unit, was undertaken by the DARPA/Tri-Service Epitaxy Characterization Team. Several wafers with epitaxial layers were measured in the same manner as substrates. The difficulty with these measurements, however, was that most of the samples had a large density of growth defects which act as point scatterers. The density was large enough so that there was usually at least one defect under the incident beam at every spot on the surface. Thus, the raster scan maps were

dominated almost entirely by the point scatterers. This is useful information, but it is difficult to extract the number of scatterers in each data point, and almost no information is obtained about the properties of the surface between the growth defects. Further work is required in conjunction with other measurements to make light scattering useful on epitaxial materials with high defect densities.

Beyond the scope of this work unit's time span, scattering measurements have continued to be made for other GaAs characterization programs. Results of these measurements have been and will be reported elsewhere.

## 9. SURFACE PREPARATION STUDIES

Surface preparation is extremely important for light scattering measurements. Since the primary sources of scattered light from specular surfaces are roughness and contamination, one must be able to separate the effects of each. This usually comes down to finding a cleaning method that is capable of removing contamination without changing the topography of the surface. Measurements before and after cleaning can then account for the relative contribution of each scatter source. Another reason for developing surface preparation methods is to have a consistent way of preparing surface for scatter measurements when the past history of a sample is unknown. In this case, differences in contamination level will not bias the results when comparing samples.

Unfortunately, it is never possible to be certain how effective a cleaning procedure is unless controlled contamination studies are performed. These studies require that a particular material surface with a particular polishing process be put through a series of tests in which samples are intentionally contaminated with particulates, films, or residues, and then cleaned until the scatter level returns to the baseline value. The baseline value is either the scatter level for a new, pristine surface, or it is the lowest scatter level obtainable by a particular cleaning process prior to intentional contamination.

Several such studies were performed during the course of this work unit. Previous publications by Stowell, et al.,<sup>7,8</sup> and standard practices in place at the early part of this work unit pointed out the effectiveness of collodion strip cleaning as a surface preparation method. However, no details of a controlled study were available, only practical experience in the lab. The controlled studies did verify the effectiveness of collodion and other strip cleaners, the details of which have been published elsewhere.<sup>13,14</sup>

It should be noted, however, that only robust surfaces stand up to repeated cleaning by

strip cleaning methods. Si is quite robust, but GaAs is not. GaAs appears to undergo some kind of roughening as a result of only a single pass of collodion.<sup>14</sup> To date, no satisfactory cleaning method has been found for GaAs once it has been contaminated. Standard practice calls for measuring GaAs in a clean environment, as received, fresh from the manufacturer's package in order to obtain reliable and consistent results.

## 10. OTHER INSTRUMENTATION

Although the scatterometer has been the workhorse of this work unit, other instruments have played an important role in the surface analysis work described in this report. These instruments include a differential interference contrast (DIC) microscope, an interferometric microscope, and a scanning probe microscope.

### 10.1 DIC Microscope

A Leitz Ortholux II POL-MK DIC microscope has been used throughout this work unit as a primary inspection tool for qualitative analysis of surfaces. With experience, even subtle fine texture of surfaces can be observed with this instrument. Magnifications of 200x, 500x, and 1000x are available, although the subtle interference contrast is often easier to see at lower magnifications. Indeed, magnifications lower than 200x have been suggested as a means to see some of the residual texture on GaAs wafers. It has always been a goal of this work unit to correlate scatter with surface properties such as roughness, and the DIC microscope will continue to play a role in this endeavor.

The DIC microscope would be more useful with lower magnification objectives, perhaps a 10x and a 5x objective which would give total magnifications of 100x and 50x respectively in combination with the 10x eyepiece. Lower magnifications can be helpful in getting a larger view of long range texture and long linear features such as shallow polishing scratches. A larger and more sophisticated sample translation stage would also increase the usefulness of the instrument. Currently, it is not possible to completely translate a 3" diameter or larger wafer under the objectives.

## 10.2 Interferometric microscope

An early model of interferometric microscope made by Zygo has been available for surface analysis. This instrument is capable of obtaining three-dimensional (3D) surface topographical measurements of surfaces within certain limits. It functions as an adjunct to scatter measurements by providing topographical information. The instrument is limited in its resolution of lateral surface features to about 0.5  $\mu\text{m}$ . It has vertical resolution better than 1 nm.

## 10.3 Scanning Probe Microscope

In late 1989, a NanoScope II scanning probe microscope (SPM) made by Digital Instruments was added to the surface analysis instrumentation. The new technology of scanning probe instrumentation offers vertical and lateral resolution on about the same order of magnitude, overcoming the limitation of the interferometric microscope and other optical based instruments which are restricted in their resolution by the diffraction limit of light. The resolution of scanning probe microscopes can be as less than 0.01 nm.

At first, the only available imaging mode was that of scanning tunneling, which can image only conducting materials. Later upgrades added the capability of atomic force imaging. New modes of scanning probe imaging are being developed every year and these new capabilities continue to be added to existing equipment as the need arises. It is beyond the scope of this report to explain the capabilities of scanning probe instrumentation, but its primary value is to provide high resolution 3D images of surfaces. These images can then be correlated with other surface analysis measurements.

The major drawback of scanning probe microscopes is the trade-off between high resolution and small field of view. The effective magnification is so high that the area of a surface probed by the laser spot of the scatterometer is on the order of 10 times larger than the largest scan size of the scanning probe microscope. Therefore, it is important to maintain an instrument,

like a scatterometer, which can measure a physical parameter proportional to surface topography over large surface areas while having the ability to probe small areas with the detail afforded by a scanning probe microscope.

## 11. MISCELLANY

### 11.1 Reference materials

The type of scatterometer described in this report requires the use of a reference material to obtain a scale factor for converting subsequent measurements to BRDF units. The reference material must have known scattering properties, and diffuse scatterers make the best reference materials for this purpose. For Lambertian scatterers, the BRDF is  $\rho/\pi$  for all scatter angles where  $\rho$  is the hemispherical reflectance.<sup>15</sup> Such reference materials are available from commercial sources with varying approximations to ideal Lambertian characteristics.

The reference material used initially was a barium sulfate plaque, which is a diffuse white material with a very good approximation to an ideal Lambertian scatterer. This reference had several disadvantages, however. The material itself is soft, like chalk. Therefore it is easily damaged by handling. The plaque was square, and the procedure spelled out for the original VAS was to attach the plaque to the sample mount via double-sided tape. Furthermore, the hemispherical reflectance of this material is approximately 0.99, which means that the theoretical BRDF is  $0.99/\pi = 0.315 \text{ str}^{-1}$ , 5-6 orders of magnitude larger than many of the very smooth materials measured on the scatterometer

The drawbacks of the barium sulfate plaque were partially addressed by a new set of reference materials available from Labsphere, Inc. The material trade name is Spectralon and it is a machinable thermoplastic with much greater durability and chemical inertness than barium sulfate. A set of four Spectralon diffuse reflectance standards was obtained with the hemispherical reflectances of 0.99, 0.75, 0.50, and 0.02. All of these reflectance standards have excellent Lambertian behavior except for small deviations at high scatter angles for the lower reflectance references. They come certified and traceable to NIST. The standards are disk shaped in a protective aluminum ring which allows for easy mounting in the standard sample

holders. In addition, the 0.02 reflectivity standard allows for reference measurements to be made at scatter levels two orders of magnitude lower than 0.99 reflectivity reference materials.

The hemispherical reflectance of the reference standard would be irrelevant if the detector linearity was perfect over a large dynamic range. The Photo Research Pritchard photometer is capable of covering a large dynamic range, but part of that range requires the use of internal neutral density filters for high signal levels. Using the 0.02 reflectivity reference standard, a reference scan can be made with photometer settings closer to those used for low scatter samples, thus reducing errors in the computed scale factor due to detector nonlinearities.

A related issue concerning the photometer's neutral density filters is worth noting here. Rotating the filter turret wheel causes the photometer's power-of-ten display to change to correspond to the increase or decrease in attenuation by the filter so that the total signal level remains unchanged. However, the automatic compensation circuitry is not perfect and drifts with time. Trim potentiometers inside the photometer can be adjusted so that the same signal level is obtained for all neutral density settings within the limits of noise. Properly trimmed, the photometer is quite linear. But if the compensation circuitry is off, performing a reference scan with a different neutral density filter than that used for a sample scan can cause significant errors. It would be best to perform the reference scan with the same neutral density filter used for a sample measurement, but this is not quite possible with the current combination of available reference materials and photometer settings.

At the time of this writing, it is still an open issue as to how accurate low scatter measurements are, considering the fact that reference scans are generally made at scatter levels several orders of magnitude higher than sample measurements. NIST is currently working on the development of low scatter reference materials, and these will be evaluated if they become available.

## 11.2 Alignment

Many references to sample alignment and system alignment have been made throughout this report. These alignment procedures are extremely important to the proper functioning of the scatterometer and to the maintenance of measurement accuracy and repeatability.

Since the definition of BRDF contains geometric quantities, a scatterometer used to measure BRDF must maintain a high degree of geometric alignment in order to properly specify such geometric terms as scatter angle and detection solid angle. The alignment procedures for the scatterometer are a complex set of steps that brings four system axes to a common intersection, which in turn defines the measurement point. The original procedures, entitled "Variable Angle Scatterometer Alignment Procedures," were written by the contractors of VTI, Inc., who built the original VAS, under contract F33615-79-C-1813.

These alignment procedures have been modified somewhat over the course of this work unit, and improvements and simplifications of the procedures will continue. An updated version of these alignment procedures will be documented in the future.

## 11.3 Standard operating procedures

Over the time span of this work unit, many changes in instrumentation, software, and alignment procedures have occurred. As a result, currently documented standard operating procedures are no longer relevant. A completely new set of standard operating procedures for system alignment, sample alignment, measurement, and data analysis is required. These procedures will either have to be passed on through training or new documentation.

## 11.4 Support for various extramural projects

Many times during the course of this work unit, requests were honored for surface

analysis on a diverse range of materials. Samples included polished metal mirrors, glass substrates, dielectric coatings, nonlinear optical materials, textured Si wafers, as well as semiconductor substrates and epitaxial material. In general, the analysis data was simply supplied to those requesting the measurements; however, a significant amount of consulting typically occurred which included data interpretation and suggestions for further study of the materials. In the process of measuring a diversity of materials, the range of applicability of the surface analysis instrumentation increased.

## 12. FUTURE DIRECTIONS

At the time of this writing, the scatterometer and its associated equipment continue to be used to characterize material surface properties and to generally support the characterization requirements of WL/AADP. Ongoing effort will likely continue in several areas, such as new substrate materials, larger samples, and analysis of the current state of the art of standard semiconductor substrates. In addition, many things unique to the technique of scatterometry, and surface analysis in general, will continue to be investigated, such as low scatter reference materials, optical alignment, automation, measurement and analysis schemes, and new designs when current instrumentation no longer satisfies new requirements.

A recent issue in this area involves substrates for high temperature devices. The wide bandgap of GaN-based devices is desirable for devices which can operate at higher temperatures than current state-of-the-art microelectronic devices. GaN epitaxial layers for these devices require a nominally lattice-matched substrate. Virtually all new substrate candidates are transparent to visible wavelengths. Converting or upgrading the scatterometer to use a UV laser source would be one option to pursue in order to apply scatterometry to these new substrate materials.

A requirement to measure polish uniformity of increasingly larger diameter substrates is expected to continue, necessitating implementation of new designs. Faster data acquisition, processing, and analysis will be required in order to characterize these larger substrates.

### 13. REFERENCES

1. Fred E. Nicodemus, "Directional Reflectance and Emissivity of an Opaque Surface," *Appl. Opt.*, Vol. 4, p. 767 (1965).
2. F. E. Nicodemus, et al., *Geometric Considerations and Nomenclature for Reflectance*, U.S. Dept. of Commerce, Washington, D.C., NBS Monograph 160 (1977).
3. J. C. Stover, *Optical Scattering: Measurement and Analysis*, McGraw-Hill, Inc., New York, p. 14 (1990).
4. H. E. Bennett and J. O. Porteus, "Relation between Surface Roughness and Specular Reflectance at Normal Incidence," *J. Opt. Soc. Am.*, Vol. 15, p. 123 (1961).
5. Fred D. Orazio, Jr., W. Kent Stowell, and Robert M. Silva, "Instrumentation of a Variable Angle Scatterometer (VAS)," *Scattering in Optical Materials*, Solomon Musikant, Editor, Proc. SPIE 362, pp. 165-171 (1982).
6. Robert M. Silva, Fred D. Orazio, Jr., and W. Kent Stowell, "Scatter Evaluation of Supersmooth Surfaces," *Generation, Measurement, and Control of Stray Radiation III*, Robert P. Breault, Editor, Proc. SPIE 384, pp. 2-9 (1983).
7. W. Kent Stowell, Robert M. Silva, and Fred D. Orazio, Jr., "Damage Susceptibility of Ring Laser Gyro Class Optics," *Generation, Measurement, and Control of Stray Radiation III*, Robert P. Breault, Editor, Proc. SPIE 384, pp. 73-79 (1983).
8. W. Kent Stowell and Fred D. Orazio Jr., "Damage Effects Identified by Scatter Evaluation of Supersmooth Surfaces," *Optical Specifications: Components and Systems*, ??, Editor, Proc. SPIE 406, pp. 23-42 (1983).
9. J. C. Stover, *Optical Scattering: Measurement and Analysis*, McGraw-Hill, Inc., New York, p. 5 (1990).
10. J. C. Stover, *Optical Scattering: Measurement and Analysis*, McGraw-Hill, Inc., New York, p. 70 (1990).
11. Thomas A. Leonard and Michael Pantoliano, "BRDF Round Robin," *Stray Light and Contamination in Optical Systems*, Robert P. Breault, Editor, Proc. SPIE 967, pp. 226-235 (1989).
12. J. L. Brown, "Light scatter variations with respect to wafer orientation in GaAs," in *Optical Scatter: Applications, Measurement, and Theory*, John C. Stover, Editor, Proc. SPIE 1530, pp. 299-305, (1991).
13. J. L. Brown, "Preparing Samples for Scattering Measurements - A Cleaning Study," *Surface Roughness and Scattering Technical Digest*, 1992, (Optical Society of America, Washington, D.C., 1992), Vol. 14, pp. 32-34.
14. J. L. Brown, "Preparing samples for scattering measurements - a cleaning study: Part 2," in *Optical Scattering: Applications, Measurement, and Theory II*, John C. Stover, Editor, Proc. SPIE 1995, pp. 80-91, (1993).
15. J. C. Stover, *Optical Scattering: Measurement and Analysis*, McGraw-Hill, Inc., New York, p. 157 (1990).